

## Bond Strength Deterioration of Reinforced and Prestressed Concrete Members at Reversed Cyclic Loads

J.-Y. Lee,<sup>a,1</sup> K.-H. Kim,<sup>b</sup> S.-W. Kim,<sup>b</sup> and H. Choi<sup>c</sup>

<sup>a</sup> Department of Civil, Architectural, and Environmental System Engineering, Sungkyunkwan University, Suwon, Republic of Korea

<sup>b</sup> Department of Architectural Engineering, Kongju National University, Kongju, Republic of Korea

<sup>c</sup> Samsung C&T, Engineering and Construction Group, Republic of Korea

<sup>1</sup> jungyoon@skku.edu

*The bond strength of concrete members at reversed cyclic loads is quite different from that of the concrete members at monotonic loads. Reversed cyclic loads produce a progressive bond deterioration that can lead to failure at cyclic stress levels lower than the ultimate stress at monotonic loads. In addition, the structural behavior of concrete members at dominant reversed loads reveals a dramatic reduction of energy dissipation in the hysteresis region due to a severe pinch effect. A method was proposed to predict the structural behavior of concrete members failing in bond after flexural yielding. The method takes into account the bond deterioration due to the degradation of concrete in the postyield range. To verify the bond behavior by the proposed method, predicted results were compared with the experimental data for concrete members at reversed cyclic loads, cited in the literature. Comparison of the experimental and calculated bond behavior of examined concrete members showed reasonable agreement.*

**Keywords:** reversed cyclic load, flexural bond strength, shear bond strength, bond strength deterioration, concrete structures.

**Introduction.** Good performance of a reinforced concrete requires an adequate interfacial bond between the reinforcing material and the concrete because the load applied must be transferred from the matrix to the reinforcement. Although the bond behavior of the steel bars in concrete subjected to monotonic load has been established and clearly addressed in various design codes, direct application of the codes to the bond strength deterioration and deformability of concrete members subjected to reversed cyclic load would be erroneous, insofar as the bond behavior of reinforced and prestressed concrete members subjected to reversed cyclic load is expected to vary from that of concrete members subjected to monotonic load. The variation arises from the fact that the bond behavior of concrete members subjected to reversed cyclic load is controlled by the key parameters, such as load patterns, length of a plastic hinge, failure modes, and flexural yielding, which are different from those of the concrete members subjected to monotonic loading. The accumulation of bond damage of a concrete member subjected to repeated or cyclic loading is assumed to be caused by the propagation of microcracks and progressive crushing of concrete in front of the lugs. The bond degradation primarily depends on the peak slip in the previous direction. Other significant parameters are: rib pattern, concrete strength, confining effects, number of loading cycles, and the peak value of slip. Hence, a deeper insight into the bond behavior of reinforced and prestressed concrete members subjected to reversed cyclic loading is required [1].

In the reinforced concrete buildings, bond failures via flexural yielding are more frequently observed during seismic events than those due to bending moments. The behavior of reinforced concrete members, which is dominated by bond or shear action, reveals a drastic reduction of energy dissipation in their hysteretic response due to strong

pinch effects. After flexural yielding, plastic hinges develop near both ends of these beams, while the reversed cyclic loading produces a progressive deterioration of bond that may lead to failure at cyclic bond stress levels lower than the ultimate stress under monotonic loading. In addition, flexural bond stress increases with the plastic hinge length induced by positive and negative loads [1]. Ichinose revealed the effect of axial force and load patterns on the bond strength of reinforced concrete columns and proposed a method to prevent the bond failure in reinforced concrete columns [2]. Lee and Watanabe studied the strength deterioration of reinforced concrete beams under cyclic load and proposed a method to predict the deformability of reinforced concrete beams failing in shear after flexural yielding [3]. However, they failed to predict the structural behavior of reinforced concrete members failing in bond. Masuo proposed formulas for evaluating the ultimate strength of reinforced concrete members subjected to antisymmetrical bending moment taking into account the splitting bond strength [4]. For concrete reinforced by steel bars, many studies have been conducted on the bond stress vs. slip curves of reinforcement in the concrete structures. Eligenhausen et al. [5] and Harajli et al. [6] proposed models to predict the bond stress vs. slip curves of steel bars in concrete subjected to monotonic or cyclic loading. In addition, Bazant et al. [7, 8] reported that the bond strength decreased with the increasing of bar diameter, and Morita et al. [9] found that the influence of the bar size on the bond strength was reduced by the constraint effect of transverse reinforcement. The bar size is considered as a critical parameter in calculation of the development length of deformed steel bars in the ACI-318 design code [10]. However, these studies provided no method to predict the bond strength deterioration of reinforced concrete members subjected to reversed cyclic loading.

In this study, a method is proposed to predict the structural bond behavior of concrete members under reversed cyclic loading.

**Flexural Bond Failure Mechanism.** Figure 1 shows a reinforced concrete beam failing in bond after flexural yielding. It also shows the crack pattern and the stress distribution of steel bars along the span of the beam subjected to an antisymmetric moment distribution. When a reinforced concrete beam is subjected to bending moment, the difference of stresses in the flexural steel bar causes bond stress ( $\tau_f$ ). From the balance of forces, the bond stress ( $\tau_f$ ), which is the rate of force variation in the reinforcing bars, can be derived as

$$T + \tau_f (pdx) = T + dT, \quad (1)$$

where  $T$  is the tensile force of the longitudinal bars,  $dT$  is the incremental tensile force of the longitudinal bars,  $dx$  is infinitesimal length of beam,  $p$  is the perimeter of steel section, taken as  $p = \pi d_t$ , and  $d_t$  is the steel bar diameter.

Therefore, the bond stress ( $\tau_f$ ) can be calculated from Eq. (1) as

$$\tau_f = \frac{dT}{pdx}. \quad (2)$$

When a concrete member is subjected to an antisymmetric moment distribution,  $dT$  is the sum of the tensile ( $T$ ) and compressive ( $C_s$ ) forces of the longitudinal bars. Thus, the bond stress of concrete members subjected to a seismic load is

$$\tau_f = \frac{T + C_s}{lp}. \quad (3)$$

where  $l$  is the bond length.

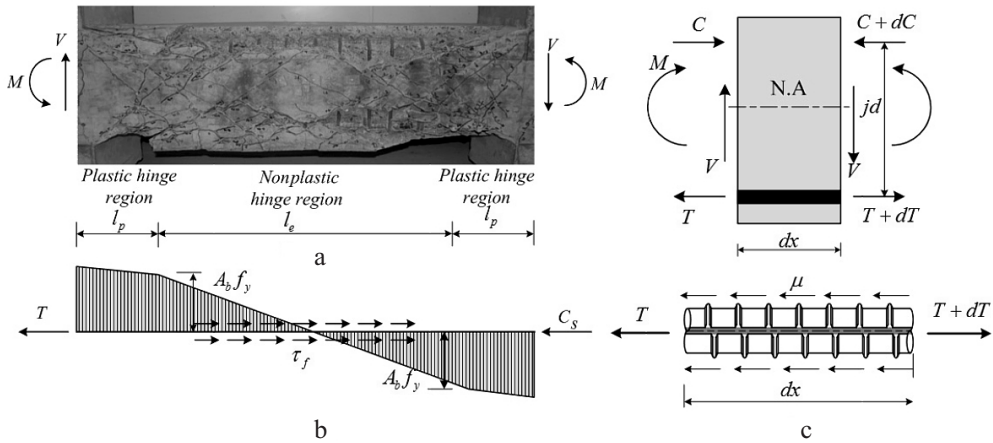


Fig. 1. Failure of a reinforced concrete beam in bond: (a) a beam subjected to reversed cyclic loading; (b) stress distribution in the steel bar; (c) forces at the infinitesimal length  $dx$ .

Before the beam attains its flexural strength, the bond length in Eq. (3) is equal to the beam length. However, when plastic hinges develop at both ends of the beam after flexural yielding, the bond length ( $l$ ) is reduced to the effective bond length ( $l_e$ ), i.e., the beam length minus the plastic hinge length ( $l_p$ ). As a result of the bond length reduction, the flexural bond stress ( $\tau_f$ ) along the longitudinal reinforcing bar increases to the following value:

$$\tau_f = \frac{T + C_s}{l_p} = \frac{A_b df_s}{l_e p}, \quad (4)$$

where  $A_b$  is the cross-sectional area of the steel bar.

After plastic hinges develop near both ends of the beam, the tensile stress,  $f_s$ , of the steel bar in Eq. (4) reaches the yield stress value ( $f_y$ ), while the compressive stress of the steel bar attains approximately the value of  $0.7f_y$  [11]. Therefore, the stress,  $df_s$ , in Eq. (4) can be replaced by the yield stress of the steel bar,  $1.7f_y$ ,

$$\tau_f = \frac{A_b (1.7f_y)}{(l - 2l_p)p}. \quad (5)$$

**Shear Bond Failure Mechanism.** The bond failure of concrete members is also influenced by a shear force. After the appearance of the 45-degree truss model by Ritter [12] and Morsch [13] at the turn of the twentieth century, there had been efforts to predict both shear strength and shear deformations using the equilibrium and compatibility conditions. In the truss model, the longitudinal reinforcement and transverse reinforcement are considered as the tensile chords of the truss, and the diagonal concrete strut as a compressive chord. Based on these findings, other compatibility-aided truss models, such as the modified compression field theory [14], the rotating angle softened truss model [15], and the fixed-angle softened truss model, were developed. In accordance with these truss models, the stresses in a reinforced concrete element are defined by the following three equilibrium equations:

$$\sigma_l = \sigma_l^c + \rho_l f_l, \quad (6)$$

$$\sigma_t = \sigma_t^c + \rho_t f_t, \quad (7)$$

$$\tau_{lt} = \tau_{lt}^c. \quad (8)$$

Here the three concrete stresses ( $\sigma_l^c$ ,  $\sigma_t^c$ , and  $\tau_{lt}^c$ ) in the  $l-t$  coordinate system can be related to the principal stresses of concrete ( $\sigma_d$  and  $\sigma_r$ ) in the  $d-r$  coordinate system using the stress transformation principle, and Eqs. (6)–(8) can be reduced to

$$\sigma_l = \sigma_d \cos^2 \alpha + \sigma_r \sin^2 \alpha + \rho_l f_l, \quad (9)$$

$$\sigma_t = \sigma_d \sin^2 \alpha + \sigma_r \cos^2 \alpha + \rho_t f_t, \quad (10)$$

$$\tau_{lt} = (-\sigma_d + \sigma_r) \sin \alpha \cos \alpha, \quad (11)$$

where  $\sigma_l$  and  $\sigma_t$  are the stresses in the reinforced concrete element in the  $l$  and  $t$  directions, respectively,  $\sigma_l^c$  and  $\sigma_t^c$  are the stresses on the concrete element, respectively,  $\tau_{lt}$  is the shear stress on the reinforced concrete element in the  $l-t$  coordinate,  $\tau_{lt}^c$  is the shear stress on the concrete element,  $f_l$  and  $f_t$  are the average steel stresses in the  $l$  and  $t$  directions, respectively,  $\rho_l$  and  $\rho_t$  are the steel ratios in the  $l$  and  $t$  directions, respectively,  $\sigma_d$  and  $\sigma_r$  are the average normal stresses of concrete in the  $d$  and  $r$  directions, and  $\alpha$  is the angle formed between the direction of the principal compression stress of concrete and the longitudinal steel direction.

In order to realize a truss mechanism, bond stress,  $\tau_{lt}$ , required for this mechanism must be smaller than bond strength. The bond stress required for the truss mechanism realization is obtained from the equilibrium of forces

$$\tau_{lt} = \frac{V}{pjd} = \frac{(\sigma_d \cos^2 \alpha - \sigma_r \sin^2 \alpha)b}{p}, \quad (12)$$

where  $V$  is shear force taken as  $V = \tau_{lt}(bjd)$ ,  $b$  is the section width, and  $jd$  is the lever arm.

#### Calculation Method of Bond Deformability.

*Step 1:* At the first step, the properties and geometric features of the specimens are input into the algorithm with the member rotation,  $R_m$ , which is defined as  $R_m = \delta/l$ , where  $\delta$  is the deflection and  $l$  is the concrete member length.

*Step 2:* The axial strain,  $\varepsilon_l$ , in the plastic hinge region of a given concrete members subjected to reversed cyclic load is calculated in the second step. Lee and Watanabe [16] proposed the following equation to evaluate the axial strain for the envelope curve:

$$\varepsilon_l = \frac{(R_{mp} + R_{mn})jd}{2l_h}, \quad (13)$$

$$l_p = 0.5 \left( \frac{M}{Vh} \right) d \quad (0.75d \leq l_p \leq d), \quad (14)$$

where  $R_{mp}$  and  $R_{mn}$  are positive and negative rotations of the concrete beam, respectively,  $l_p$  is the length of the plastic hinge region,  $M/(Vh)$  is the shear span-to-depth ratio, and  $d$  is the beam effective depth.

*Step 3:* At the third step, the slip of steel bar ( $S$ ) is calculated. Before the flexural yielding of the beam, the strain distribution changes almost linearly along the member, while after the flexural yielding the steel strain in the plastic hinges of the beam abruptly increases because of the strain accumulation of the longitudinal steel bars. The analytical results of the displacement-based assessment of reinforced concrete frames in earthquakes by Bonacci and Wight [17] indicated that the share of anchorage in deformation increased with the story drift. After plastic hinges develop at both ends of the beam, the pullout slip of the beam steel bars in the joint panel can be calculated as

$$S = \int_0^l (\varepsilon_s - \varepsilon_c) dx, \tag{15}$$

where  $\varepsilon_s$  is the strain of steel bars and  $\varepsilon_c$  is the strain of concrete. Since large inelastic deformations are likely to occur in the interior joints, the contribution of the concrete strains to the relative slip is negligible. Thus, Eq. (15) becomes

$$S = \int_0^l \varepsilon_s dx. \tag{16}$$

*Step 4:* The bond strength of concrete members subjected to reversed cyclic load is calculated at Step 4. Repeated or cyclic loads produce a progressive deterioration of bond that may lead to failure at cyclic bond stress levels lower than the ultimate stress under monotonic load. The accumulation of bond damage is supposed to be caused by the propagation of microcracks and progressive crushing of concrete in front of the lugs [5]. Cycles with reversed load produce degradation of bond strength and bond stiffness that is more severe than those at the same number of load cycles with a unidirectional repeated load. Degradation primarily depends on the peak slip in either direction reached previously. Other significant parameters are rib pattern, concrete strength, confining effects, number of load cycles, and peak value of slip, between which the bar is cyclically loaded.

The analytical models of the local bond stress-slip relationship for cyclic load were proposed by Morita and Kaku [18], Tassios [19], and Eligehausen et al. [5]. Model [5] takes into account the main parameters that appear to control the behavior observed in the tests. Reduced cyclic envelopes are obtained from the monotonic envelope by decreasing the characteristic bond stress through reduction factors, which are formulated as a function of the so called damage parameter. In the present study, the bond strength,  $\tau_{bu}$ , proposed by Fujii and Morita [20] is used. In addition, the analytical model for bond stress vs. slip relationship of concrete [5] is applied, as follows

$$\tau_{bu} = \tau_{co} + \tau_{st}, \tag{17}$$

where  $\tau_{co}$  is the concrete contribution to the shear stress, which is derived as

$$\tau_{co} = 0.313(0.4b_i + 0.5)\sqrt{f'_c}, \tag{18}$$

$\tau_{st}$  is the reinforcement contribution to the shear stress, which in case of the corner splitting, is reduced to

$$\tau_{st} = 0.313 \frac{50A_s\sqrt{f'_c}}{sd_b}, \tag{19a}$$

and in case of the side splitting, is derived as

$$\tau_{st} = \frac{0.313}{sd_b} \left( \frac{40}{N_t} + \frac{10N_u}{N_t} + \frac{30N_s}{N_t} \right) A_s \sqrt{f'_c}, \quad (19b)$$

where  $b_i$  is the coefficient related to the bond failure mode,  $f'_c$  is the compressive strength of concrete,  $A_s$  is the sectional area of the shear reinforcement covering the corner steel,  $N_s$  is the number of the flexural steel bars directly hooked by the supplemental ties,  $N_u$  is the number of free (not hooked) flexural steel bars, and  $N_t$  is the total number of directly hooked flexural steel bars. The values of  $\tau_{co}$ ,  $\tau_{st}$ , and  $f'_c$  in Eqs. (18), (19a), and (19b) are given in MPa.

*Step 5:* At step 5, the flexural bond stress and the shear bond stress are calculated via Eqs. (5) and (12), respectively.

*Step 6:* After the bond strength,  $\tau_{bu}$ , and flexural and shear bond stresses are calculated at Steps 4 and 5, the bond resistance and bond force is calculated as

$$V_{bu} = \tau_{bu} pjd, \quad (20a)$$

$$V_f = \tau_f pjd. \quad (20b)$$

If the value of  $V_{bu}$  is higher than the shear value,  $V_{flexure}$ , which corresponds to formation of the plastic hinge, a new value of the longitudinal axial strain is assumed and the steps are repeated until the potential shear value  $V_{bu}$  (or  $V_f$ ) equals the shear force at onset of flexural yielding,  $V_{flexure}$ . When  $V_{bu}$  (or  $V_f$ ) reaches  $V_{flexure}$ , the corresponding deflection (or rotation) assumed in Step 1 is taken as the maximum deformation,  $R_b$ , of the beam failing in bond. In case of a shear fracture mode, once a transverse strain value is attained, the analytical shear force,  $V_{lt}$ , in the beam can be assessed using the compatibility procedures of the applied truss model [14, 15].

*Step 7:* The deflection (or rotation) of the concrete members failing in bond is calculated at Step 7. The least value of the two calculated maximum deflections or rotations is taken as the ductile capacity of these members (see Fig. 2):

$$\Delta = \min[\Delta_s, \Delta_b] \quad \text{or} \quad R = \min[R_s, R_b], \quad (21)$$

where  $\Delta_s$  and  $\Delta_b$  are the maximum deflections of the reinforced concrete members failing in shear and bond, respectively, while  $R_s$  and  $R_b$  are the rotations of the reinforced concrete members failing in shear and bond, respectively. The least value of  $R_b$  and  $R_s$  is taken as the maximum deformation of the reinforced or prestressed concrete members subjected to the reversed cyclic loading.

**Testing Plan.** The proposed model to calculate the bond deformability of concrete members subjected to reversed cyclic load was verified against the observed results of four reinforced concrete beams. All tested beams were designed to fail in bond after flexural yielding [21]. The potential shear strength ratio was higher than 1. Figure 3 shows the overall dimensions, arrangement of reinforcement, as well as the loading setup. Each tested specimen consisted of two regions: a test region of 1200 mm long and a loading region consisting of two loading stubs, 400 mm long. Heavier reinforcement was placed outside the test region to prevent a premature failure in the stub zones.

The tested beams were 200 mm wide and 300 mm deep. The specimens were loaded with an antisymmetric moment distribution using a hydraulic jack and a servo actuator, as shown in Fig. 3. The compressive strength of concrete was assessed as 29.3 MPa. Table 1

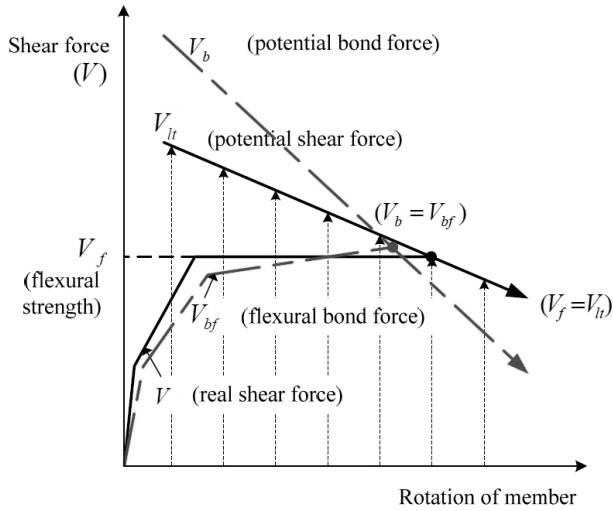


Fig. 2. Deformability of reinforced or prestressed concrete members subjected to reversed cyclic loading.

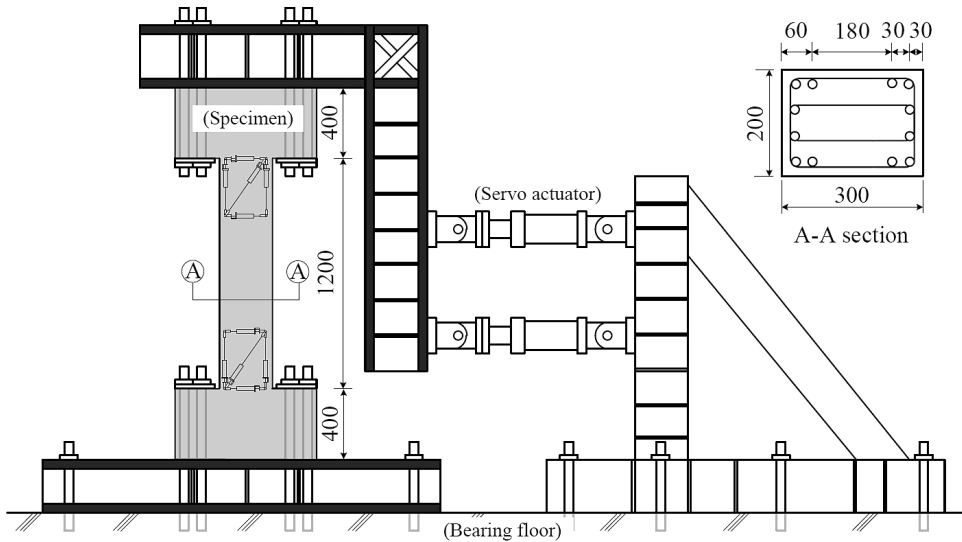


Fig. 3. Test specimen and loading system [21].

shows the material properties of the beams in details. Further details about the tested beams and the test procedures can be found elsewhere [21].

The specimens were loaded at 600 mm far from the lower stub and one plastic hinge was developed in the lower end of the beams. The schematic diagram of experimental set-up and the locations of a linear variable differential transducer (LVDT) are shown in Fig. 3. Five linear displacement transducers were attached to face of the hinge region of the test beam to measure the curvature, longitudinal and transverse axial deformation, as well as shear deformation. In addition, the strains of the transverse and longitudinal steel bars in the test region were measured by strain gauges attached to the surface of the steel bars. Two LVDTs were attached to the face of the base stub to measure the axial elongation in the stub. Four LVDTs were attached to both sides of the beams to measure the angle of rotation, the deflection, and the P-delta effect. The specimens were supported in the vertical

Table 1

Test Specimens

Member	$f'_c$ , MPa	Shear reinforcement				Longitudinal tensile reinforcement			
		$s$ , mm	$\rho_w$ , %	$A_w$ , mm <sup>2</sup>	$f_{wy}$ , MPa	$n$	$\rho_t$ , %	$A_t$ , mm <sup>2</sup>	$f_{ly}$ , MPa
BB1	29.3	82	0.390	479.70	384.0	4	1.965	884.25	435.0
BB3	29.3	80	0.800	960.00	384.0	4	1.965	884.25	435.0
BB5	29.3	143	0.224	480.48	384.0	4	1.965	884.25	435.0
BB7	29.3	108	0.593	960.66	384.0	4	1.965	884.25	435.0

Note:  $f'_c$  is the compressive strength of concrete,  $s$  is stirrup spacing,  $\rho_w$  is shear reinforcement ratio,  $A_w$  is the total area of stirrup,  $f_{wy}$  is yield stress of stirrup,  $A_t$  is area of longitudinal steel,  $f_{ly}$  is the yield stress of tensile longitudinal bar,  $n$  is the number of tensile reinforcements, and  $\rho_t$  is tensile longitudinal reinforcement ratio.

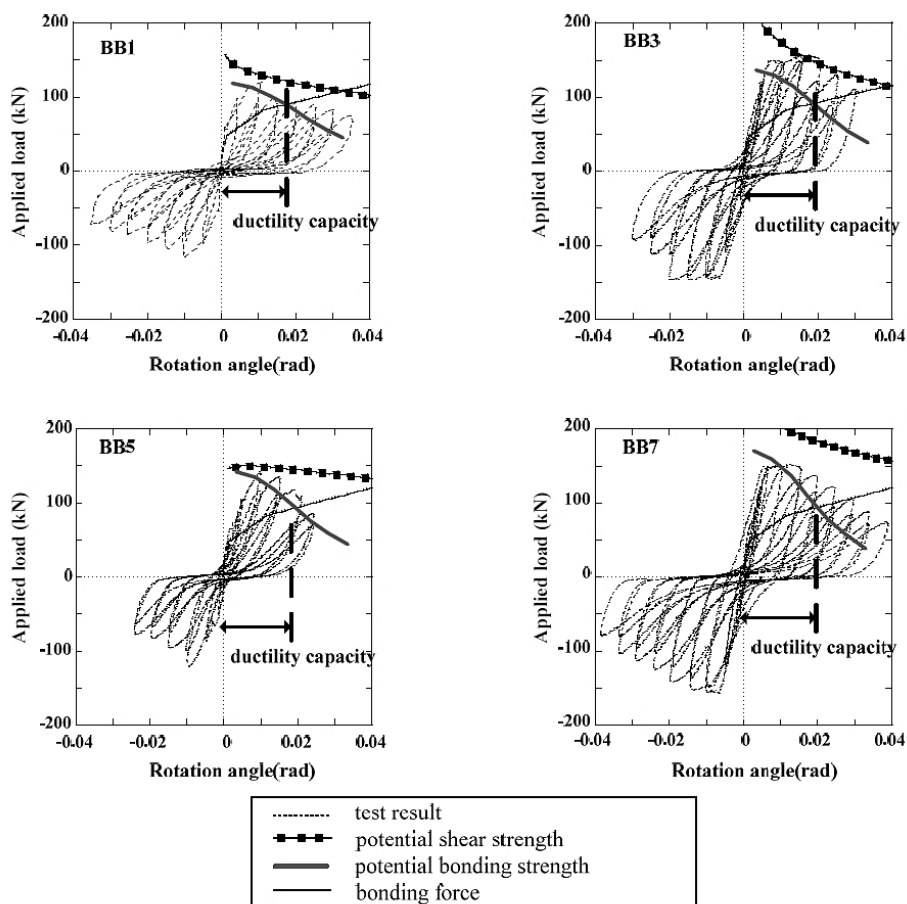


Fig. 4. Experimental and calculated load vs. rotation angle dependences.

position, and quasi-static cyclic lateral load was applied to the top of the column using a servo-controlled hydraulic actuator. A lateral cyclic load was applied under displacement control by a horizontal actuator with the displacement capacity of  $\pm 400$  mm. To prevent

any displacement in the out-of-plane direction, four rollers were applied. In the test, a strain-controlled test procedure was adopted. The test was terminated when the resisting force in the post-peak load-deformation curve dropped to about 80% of the recorded peak strength.

**Ductility Capacity Prediction.** All tested specimens failed in bond after flexural yielding. The first minor flexural cracks appeared about 30 kN in the lower part of the member. Flexural yielding was observed at a drift ratio of approximately 0.8%. Cracks and concrete spalling were observed in the plastic hinge region after the flexural tensile steel bars reached their yield stress values. Failure of all tested specimens occurred by the bond mechanism, while no cases of longitudinal bar buckling were observed.

Figure 4 shows the predicted and experimental load versus rotation responses for four specimens, where the predicted deformability was obtained according to the calculation procedure. The potential shear and bond strength of the truss mechanism are gradually reduced with the rotation angles. When the potential bond strength reaches the respective bond stress value, the corresponding deflection (or rotation) assumed at step 1 is taken as the maximum deformation of the beam. The results obtained show that the proposed method predicted the bond deformability of the reinforced concrete members with a standard deviation of 1.27 and covariance of 14.2%.

**Conclusions.** In the concrete buildings, bond failures after flexural yielding are frequently observed rather than bending moments during seismic events. In this study, a method was proposed to predict the structural behavior of reinforced and prestressed concrete members failing in bond after flexural yielding. From the analytical and experimental investigations, the following conclusions can be drawn.

1. A bond ductility evaluation method for concrete members subjected to reversed cyclic loading was proposed with consideration of the degradation of bond strength due to the accumulation of bond damage.

2. The proposed method was compared to the experimental results of four reinforced concrete members failing in bond. Using this approach, the bond deformability of the tested concrete members was predicted with a reasonable accuracy.

3. However, additional efforts are required for studying the effect of strength deterioration at large rotation angle values to predict more accurately the ductile capacity of concrete members failing in bond after flexural yielding.

**Acknowledgments.** This research was supported by Basic Science Research Program through the National Research Foundation of Korea (NRF) funded by the Ministry of Education (2013006697).

1. J.-Y. Lee, H. Choi, and J.-Y. Lim, "Bond deformability of reinforced concrete members," in: Proc. of the 15th World Conf. on *Earthquake Engineering*, Lisbon, Portugal (2012), 10 p.
2. T. Ichinose, "Splitting bond failure of columns under seismic action," *ACI Struct. J.*, **92**, No. 5, 535–542 (1995).
3. J.-Y. Lee and F. Watanabe, "Shear deterioration of reinforced concrete beams subjected to reversed cyclic loading," *ACI Struct. J.*, **100**, No. 4, 480–489 (2003).
4. M. Masuo, "Evaluation of ultimate shear strength and yield deformation of reinforced concrete columns and beams," *Trans. AIJ*, **452**, 87–97 (1993).
5. R. Eligehausen, E. P. Popov, and V. V. Bertero, *Load Bond Stress-Slip Relationships of Deformed Bars under Generalized Excitations*, Report No. UCB/EERC82-83, Earthquake Engineering Research Center, University of California, Berkeley, CA (1983).
6. M. H. Harajli, B. S. Hamad, and A. A. Rteil, "Effect of confinement of bond strength between steel bars and concrete," *ACI Struct. J.*, **101**, No. 5, 595–603 (2004).

7. Z. P. Bažant and R. Desmorat, "Size effect in fiber or bar pullout with interface softening slip," *J. Eng. Mech.*, **120**, No. 9, 1945–1962 (1994).
8. Z. P. Bažant, Z. Li, and M. Thoma, "Identification of stress-slip law for bar or fiber pullout by size effect tests," *J. Eng. Mech.*, **121**, No. 5, 620–625 (1995).
9. S. Morita, S. Fuji, and G. Kondo, "Experimental study on size effect in concrete structures," in: H. Mihashi, H. Okamura, and Z. P. Bažant (Eds.), *Size Effect in Concrete Structures*, E&FN Spon, London (1994), pp. 21–40.
10. *ACI 318-11: Building Code Requirements for Structural Concrete and Commentary*, American Concrete Institute, Farmington Hills, MI (2011).
11. T. Paulay and M. J. N. Priestley, *Seismic Design of Reinforced Concrete and Masonry Buildings*, John Wiley and Sons, New York (1992).
12. W. Ritter, "Die Bauweise Hennebique," *Schweiz. Bauzeit.*, **33**, No. 7, 59–61 (1899).
13. E. Morsch, "Versuche über Schubspannungen in Betoneisenträgern," *Beton und Eisen*, **2**, No. 4, 269–274 (1903).
14. F. J. Vecchio and M. P. Collins, "The modified compression-field theory for reinforced concrete elements subjected to shear," *ACI Struct. J.*, **83**, No. 2, 219–231 (1986).
15. T. T. C. Hsu, "Softened truss model theory for shear and torsion," *ACI Struct. J.*, **85**, No. 6, 624–635 (1988).
16. J.-Y. Lee and F. Watanabe, "Predicting the longitudinal axial strain in the plastic hinge regions of reinforced concrete beams subjected to reversed cyclic loading," *Eng. Struct.*, **25**, No. 7, 927–939 (2003).
17. J. F. Bonacci and J. K. Wight, "Displacement-based assessment of reinforced concrete frames in earthquakes," in: Proc. of Mete A. Sozen Symp., ACI Publ. SP-162 (1996), pp. 117–138.
18. S. Morita and T. Kaku, "Local bond stress-slip relationship under repeated loading," Proc. of IABSE Symp. on Resistance and Ultimate Deformability of Structures Acted on by Well Defined Repeated Loads, Lisbon, Portugal (1973), pp. 221–227.
19. T. P. Tassios, "Properties of bond between concrete and steel under load cycles idealizing seismic actions," in: Proc. of AICAP-CEB Symp. (Apr. 1979, Rome), CEB Bull. No. 131, Paris (1979), pp. 67–122.
20. S. Fujii and S. Morita, "Splitting bond capacities of deformed bars. Part 1. Experimental studies on main factors influencing splitting bond failure," *Trans. AIJ*, **319**, 47–55 (1982).
21. J.-Y. Lee, theoretical prediction of shear strength and ductility of reinforced concrete beams, A Thesis submitted for the Degree of Doctor of Philosophy, Kyoto University (1998).

Received 20. 10. 2014